STATE-SPACE REPRESENTATIONS FOR DIGITAL WAVEGUIDE NETWORKS OF LOSSY FLARED ACOUSTIC PIPES

Rémi Mignot [*] [†] *, Thomas Hélie,*
IRCAM & CNRS, UMR 9912
1, pl. Igor Stravinsky,
75004 Paris, France
{mignot,helie}@ircam.fr

Denis Matignon
ISAE, Applied Mathematics Training Unit,
10, av. E. Belin, B.P. 54032.
F-31055 Toulouse cedex4, France
denis.matignon@isae.fr

ABSTRACT

This paper deals with digital waveguide modeling of wind instruments. It presents the application of state-space representations to the acoustic model of *Webster-Lokshin*. This acoustic model describes the propagation of longitudinal waves in axisymmetric acoustic pipes with a varying cross-section, visco-thermal losses at the walls, and without assuming planar or spherical waves. Moreover, three types of discontinuities of the shape can be taken into account (radius, slope and curvature), which can lead to a good fit of the original shape of pipe. The purpose of this work is to build low-cost digital simulations in the time domain, based on the *Webster-Lokshin* model. First, decomposing a resonator into independent elementary parts and isolating delay operators lead to a network of input/output systems and delays, of *Kelly-Lochbaum* network type. Second, for a systematic assembling of elements, their state-space representations are derived in discrete time. Then, standard tools of automatic control are used to reduce the complexity of digital simulations in time domain. In order to validate the method, simulations are presented and compared with measurements.

1. INTRODUCTION

Studying physical modeling for sound synthesis allows to simulate the behavior of musical instruments. Consequently it naturely leads to realistic sounds, especially during attacks and note transitions, compared to signal processing approaches. However, digital simulations in time domain require intensive computations from signal processors, and simplifications of the physical model have to be considered to make real-time simulations possible. Moreover, because of interactions between elements of an instrument, building a modular synthetizer proves difficult.

With the approach of digital waveguides (cf. eg. [1]), some works have considered 1D acoustic model of axisymmetric pipes based on the *Webster* horn equation (cf. [2]). Approximating a varying cross-section pipe by some cylinders or cones leads to the *Kelly-Lochbaum* scattering network (cf. eg. [3, 4]), which allows a low-cost digital simulation in time domain. These models assume planar and spherical waves respectively. For a more realistic behavior of the virtual instrument, in [5] and [6] visco-thermal losses have been taken into account. This model of losses (cf. [7]) involves fractional derivatives, and is more accurate than more standard dampings based on integer order derivatives. In [8], the *Kelly-Lochbaum* network has been derived for pipes with continuity of radius and slope ($\mathcal{C}^1$-regularity of the shape), using the *Webster-Lokshin* acoustic model of lossy flared pipes which does not assume planar or spherical waves (cf. [9]).

After modeling each piece of pipe separately, it is necessary to put them together in order to build the whole resonator. In [10] and [11], the following modular method is proposed: deriving *state-space representations* of every pieces of pipe in discrete time domain, interconnection laws allow to calculate the state-space representation of the whole resonator. This formalism facilitates the modularity of the building of a virtual trombone.

In a recent work [12], a framework (based on the *Webster-Lokshin* equation) has been derived and allows to recover all models mentioned above ([3, 5, 4, 6, 8]). Moreover, it allows to obtain a good level of accuracy with a small number of pipes. The novelty of the present work is the use of the formalism of [11], starting from the unifying model of [12]. Thanks to the modularity of the method, virtual wind instruments can be built connecting additional models such as: mouth-piece, radiation, tone-hole, lips and reed (which are not studied in this paper). For example, Fig. 1 presents the network of a possible virtual resonator built by connecting such acoustic elements.

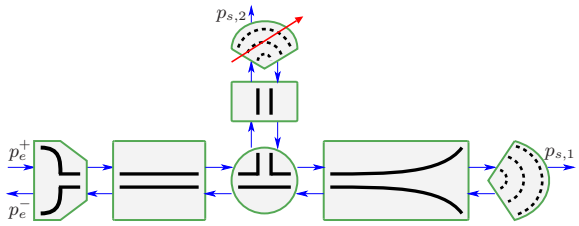

Figure 1: Example of an acoustic network modeling a resonator with a mouth-piece, a horn and a tone-hole.

This document is organized as follows. In section 3, a pipe with varying cross-section is separated into some pieces of pipe. Using the *Webster-Lokshin* model, each piece of pipe is modeled by an input/output network of the *Kelly-Lochbaum* type. In section 4, a state-space representation is derived for the network of section 2, in continuous time and in discrete time. Section 5 presents standard tools of automatic control which allow to optimize numerical realizations in order to obtain low-cost digital simulations in the time domain. Section 6 presents the digital simulations of virtual trombones and a comparison between computed impedances and the measured impedance of a real trombone. The last section concludes this paper and deals with perspectives.

[*] Rémi Mignot is Ph.D. student at Télécom ParisTech/TSI

[†] This work is supported by the CONSONNES project, ANR-05-BLAN-0097-01

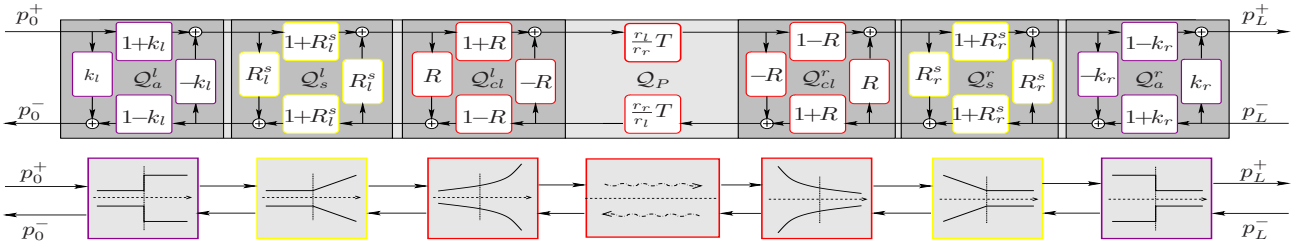

Figure 2: *Separation of the effects of pipe geometry.*

2. MODELING A PIECE OF PIPE

2.1. Webster-Lokshin model and traveling waves

The Webster-Lokshin model is a mono-dimensional model which characterizes linear waves propagation in axisymmetric pipes, assuming the quasi-sphericity of isobars near the inner wall (cf. [9, 13]), and taking into account visco-thermal losses (cf. [7]) at the wall. The acoustic pressure P and the particle flow U are governed by the following equations, given in the Laplace domain:

$$\left[\left(\left(\frac{s}{c_0}\right)^2+2\varepsilon(\ell)\left(\frac{s}{c_0}\right)^{\frac{3}{2}}+\Upsilon(\ell)\right)-\partial_\ell^2\right]r(\ell)P(\ell,s)=0, \qquad (1)$$

$$\rho_0\, s\, \frac{U(\ell,s)}{S(\ell)}+\partial_\ell p(\ell,s)=0, \qquad (2)$$

where $s\in\mathbb{C}$ is the Laplace variable, ℓ is the space variable measuring the arclength of the wall, $r(\ell)$ is the radius of the pipe, $S(\ell)=\pi r(\ell)^2$ is the section area, $\varepsilon(\ell)=\kappa_0\sqrt{1-r'(\ell)^2}/r(\ell)$ quantifies the visco-thermal losses and $\Upsilon(\ell)=r''(\ell)/r(\ell)$ is the curvature. Eq. (1) is called the *Webster-Lokshin* equation, and (2) is the *Euler* equation satisfied outside the boundary layer. The physical constants are the mass density ρ_0, the speed of sound c_0, and $\kappa_0=\sqrt{l'_v}+(\gamma-1)\sqrt{l_h}$ where l'_v and l_h denote characteristic lengths of viscous (l'_v) and thermal (l_h) effects.

With the formalism of *Digital Waveguides*, it is usual to describe acoustic effects with traveling waves rather than P and U. In this work, we define the change of variables by introducing a virtual *reference pipe*: a lossless cylinder with (arbitrary) radius r_c. Its characteristic impedance is $Z_c=\rho_0\, c_0\,/S_c$, with $S_c=\pi r_c^2$, for which corresponding planar traveling waves would be defined by

$$\begin{bmatrix}p^+(\ell,s)\\ p^-(\ell,s)\end{bmatrix}=\frac{1}{2}\begin{bmatrix}1 & Z_c\\ 1 & -Z_c\end{bmatrix}\begin{bmatrix}P(\ell,s)\\ U(\ell,s)\end{bmatrix}. \qquad (3)$$

In the case of lossy varying cross-section pipes, these variables are neither decoupled nor perfectly progressive inside the pipe. Nevertheless, they remain "physically meaningful" at interfaces of the pipe (cf. [12]), and respect the causality principle.

2.2. Two-port system of a piece of pipe

In this paper, a pipe with varying cross-section is approximated by a concatenation of pieces of pipe with constant parameters. Thus, a piece of pipe is defined as a finite pipe with length L, and with constant curvature (Υ) and losses (ε) parameters.

The piece of pipe is modeled by a system, the inputs of which are $p_0^+(s):=p^+(\ell=0,s)$ and $p_L^-(s):=p^-(\ell=L,s)$ (incoming waves at $\ell=0$ and $\ell=L$). Outputs are $p_0^+(s)$ and $p_L^-(s)$ (outgoing waves).

In [12], a detailed analysis gives a framework which represents the system of a piece of pipe. In this framework, delays and effects of geometry of the pipe are isolated from each others. The geometrical parameters are the radii at ends r_0 and r_L, the slopes at ends r'_0 and r'_L, the curvature and the visco-thermal losses of the piece of pipe (Υ and ε). The framework is presented in Fig. 2 where

$$k_l=\frac{Z_l-Z_c}{Z_l+Z_c},\quad\text{and}\quad k_r=\frac{Z_r-Z_c}{Z_r+Z_c}, \qquad (4)$$

$$R_l^s(s)=\frac{\alpha_l}{s-\alpha_l},\quad\text{with }\alpha_l=-\frac{c_0}{2}\frac{r'_l}{r_l}, \qquad (5)$$

$$R_r^s(s)=\frac{\alpha_r}{s-\alpha_r},\quad\text{with }\alpha_r=+\frac{c_0}{2}\frac{r'_r}{r_r}, \qquad (6)$$

$$R(s)=\frac{s/c_0-\Gamma(s)}{s/c_0+\Gamma(s)}, \qquad (7)$$

$$T(s)=e^{-\Gamma(s)L}=D(s)\,e^{-\frac{s}{c_0}L}, \qquad (8)$$

$$\text{with}\quad D(s)=e^{-\left(\Gamma(s)-\frac{s}{c_0}\right)L}, \qquad (9)$$

$$\text{and}\quad \Gamma(s)=\sqrt{\left(\frac{s}{c_0}\right)^2+2\varepsilon\left(\frac{s}{c_0}\right)^{\frac{3}{2}}+\Upsilon}, \qquad (10)$$

and where $\sqrt{.}$ denotes an analytical continuation of the positive square root of $\mathbb{R}^+$ on a domain compatible with the one-sided Laplace transform, namely $\mathbb{C}_0^+=\{s\in\mathbb{C}/\Re e(s)>0\}$ (see Ref. [14, 15] for more details). The function Γ is proved to be analytical in $\mathbb{C}_0^+$, and such that $\Re e(\Gamma(s))\geq 0$ if $\varepsilon\geq 0$.

Brief interpretations of cells of Fig.2 are

- Cells $\mathcal{Q}_a^l$ and $\mathcal{Q}_a^r$, with k_l and k_r (cf. (4)), remind *Kelly-Lochbaum* junctions between two lossless cylinders (cf. eg. [3, 5]) with discontinuities of sections.
- Cells $\mathcal{Q}_s^l$ and $\mathcal{Q}_s^r$, with R_s^l and R_s^r (cf. (5-6)), are similar to *Kelly-Lochbaum* junctions between lossless cones (cf. eg. [4, 6]) with discontinuities of slopes.
- Cells $\mathcal{Q}_{cl}^l$ and $\mathcal{Q}_{cl}^r$, with $R(s)$, remind *Kelly-Lochbaum* junctions between lossy pipes with constant curvature of [8].
- $T(s)$ (cf. (8)), of the cell $\mathcal{Q}_{cl}^l$, represents the delay L/c_0 of wave propagation through the piece of pipe, and the effect $D(s)$ (cf. (9)) due to the visco-thermal losses and the curvature. In [14] $D(s)$ is proved to be causal and stable.

The framework of Fig. 2 is interesting because the effects of the curvature and losses are isolated from the others (section and slope), and it makes their study easier. Because of the square roots in the function Γ (cf. (10)), the study requires special treatments (see sec. 3.1).

3. STATE-SPACE REPRESENTATION

For a systematic building of resonators, it is proposed to derive state-space representations for each cell of Fig. 2. These representations allow algebraic manipulations on the system using well-known tools of automatic control (see sec. 4). Introducing the input vector U ($N\times 1$), the output vector Y ($N\times 1$), and the state vector X ($J\times 1$), each cell is rewritten with the following representation in continuous time

$$\left\{\begin{array}{rcl} s\,X(s) &=& A\,X(s)+B\,U(s),\\ Y(s) &=& C\,X(s)+D\,U(s).\end{array}\right. \tag{11}$$

3.1. Finite-dimensional systems

Because of the square roots in $\Gamma(s)$, transfer functions such as $R(s)$ and $T(s)$ (see sec. 2.2) are irrational. These functions have continuous lines of singularities in $\mathbb{C}$, which are named *cuts*. These cuts join some points (*branching points*) and the infinity.

If $\Upsilon=0$, the function Γ has one branching point at $s=0$. The cut $\mathbb{R}^-$ is chosen to preserve the hermitian symmetry. Thereof, transfer functions have a continuous line of singularities on $\mathbb{R}^-$. The residues theorem shows that these functions are represented by a class of infinite-dimensional systems, called *Diffusive Representations* (cf. [16, 17, 15]). For any diffusive representation $H(s)$ which is analytic on $\mathbb{C}\backslash\mathbb{R}^-$:

$$H(s) = \int_0^\infty \frac{\mu_H(\xi)}{s+\xi}\mathrm{d}\xi, \tag{12}$$

$$\mu_{_H}(\xi) = \frac{1}{2i\pi}\{H(-\xi+i0^-)-H(-\xi+i0^+)\}. \tag{13}$$

For simulation in time domain, eg. in [17], it is proposed to approximate such diffusive representations by finite-dimensional approximations, given by $\widetilde{H}(s)=\sum_{j=1}^{j=L}\frac{\mu_j^H}{s+\xi_j}$, where L is the number of poles, $-\xi_j\in\mathbb{R}^-$ is the position of the jth pole and μ_j^H is its weight. The poles are placed in $\mathbb{R}^-$ with a logarithmic scale, and the weights μ_j^H are obtained by a least-square optimization in the Fourier domain.

If $\Upsilon>0$, Γ has two more branching points, which are complex conjugate. In this case, diffusive representations are approximated with a finite sum of 1st and 2nd order differential systems:

$$\widetilde{H}(s)=\sum_{j=1}^{j=L}\frac{\mu_j^H}{s+\xi_j}+\sum_{j=1}^{j=M}\left(\frac{w_j^H}{s+\gamma_j}+\frac{\overline{w}_j^H}{s+\overline{\gamma}_j}\right). \tag{14}$$

R and D can be approximated with $L+2M=10$ or 15.

3.2. State-space representations in continuous time

Cells $\mathcal{Q}_a^l$ and $\mathcal{Q}_a^r$ These Cells only contain constant coefficients k_l and k_r. With $\mathcal{Q}_a^l$ for example, the state-space representation is

$$A=[\,],\quad B=[\,],\quad C=[\,],\quad D=\begin{bmatrix}k_l & 1-k_l\\ 1+k_l & -k_l\end{bmatrix}. \tag{15}$$

A, B, C are degenerated (empty) matrices, but this convenient notation is used to standardize the procedures in the sequel.

Cells $\mathcal{Q}_s^l$ and $\mathcal{Q}_s^r$ They contain one first-order transfer function, the state-space representation of $\mathcal{Q}_s^l$ is

$$A=\begin{bmatrix}\alpha_l\end{bmatrix},\quad B=\begin{bmatrix}1 & 1\end{bmatrix},\quad C=\begin{bmatrix}\alpha_l\\ \alpha_l\end{bmatrix},\quad D=\begin{bmatrix}0 & 1\\ 1 & 0\end{bmatrix}. \tag{16}$$

Cells $\mathcal{Q}_{cl}^l$ and $\mathcal{Q}_{cl}^r$ The transfer function R of the type (12) is approximated by $\widetilde{R}$ of the type (14). The state-space representation of $\mathcal{Q}_{cl}^l$ is given by the following diagonal form

$$\begin{aligned} A &= \mathrm{diag}(\begin{bmatrix}\xi_1,\ ...,\ \xi_L, \gamma_1,\ ...,\ \gamma_M, \overline{\gamma}_1,\ ...,\ \overline{\gamma}_M\end{bmatrix}),\\ C &= \begin{bmatrix}\mu_1^R,\ ...,\ \mu_L^R, w_1^R,\ ...,\ w_M^R, \overline{w}_1^R,\ ...,\ \overline{w}_M^R\\ \mu_1^R,\ ...,\ \mu_L^R, w_1^R,\ ...,\ w_M^R, \overline{w}_1^R,\ ...,\ \overline{w}_M^R\end{bmatrix},\\ B &= \begin{bmatrix}1, & ... & 1\\ -1, & ... & -1\end{bmatrix}^T \text{ and } D=\begin{bmatrix}0 & 1\\ 1 & 0\end{bmatrix}.\end{aligned} \tag{17}$$

Cell $\mathcal{Q}_p$ In the central cell $T(s)=D(s)\,\mathrm{e}^{-\frac{L}{c_0}s}$. The transfer function $D(s)$ of type (12) is approximated by $\widetilde{D}(s)$ of type (14) for which the state-space representation can be written

$$\begin{aligned} A &= \mathrm{diag}(\begin{bmatrix}\xi_1,\ ...,\ \xi_L, \gamma_1,\ ...,\ \gamma_M, \overline{\gamma}_1,\ ...,\ \overline{\gamma}_M\end{bmatrix}),\\ C &= \begin{bmatrix}\mu_1^D,\ ...\ \mu_L^D, w_1^D,\ ...\ w_M^D, \overline{w}_1^D,\ ...\ \overline{w}_M^D\end{bmatrix},\\ B &= \begin{bmatrix}1, & ... & 1\end{bmatrix}^T \text{ and } D=\begin{bmatrix}0\end{bmatrix}.\end{aligned} \tag{18}$$

Pure delay operators are treated differently : for $\mathrm{e}^{-\tau s}$, if $\tau=MT_s$ with $M\in\mathbb{N}^*$ and T_s is the sampling period, its discrete-time version is Z^{-M} and is performed by a circular buffer. If M is fractional, interpolation filters are needed (cf. eg. [4, 11]).

3.3. State-space representations in discrete time

Since every state-space representation are written in diagonal form, the dynamics equation behaves as J independent first order equations with poles $a_j=A_{j,j}$. This leads to

$$sX_j = a_jX_j+V_j,\ \text{ for } 1\le j\le J, \tag{19}$$

where $V_j=\sum_{n=1}^N B_{(j,n)}U_n$.

Using any standard discretization schemes, J discrete-time equations of the first order are derived from (19). The corresponding difference equations are[1]

$$zX_j^d=\alpha_jX_j^d+(z\lambda_{(j,1)}+\lambda_{(j,0)})V_j^d,\ \text{for } 1\le j\le J. \tag{20}$$

With $\Lambda_l=\mathrm{diag}(\{\lambda_{(j,l)}\}_{1\le j\le J})B$ for $l\in\{0,1\}$, and $A^d=\mathrm{diag}(\{\alpha_j\}_{1\le j\le J})$, the matrix version is

$$zX^d = A^dX^d+(z\Lambda_1+\Lambda_0)U^d, \tag{21}$$

$$Y^d = CX^d+DU^d. \tag{22}$$

Equation (21), is not a standard dynamics equation of state-space representation, because x_n depends upon u_n in the time domain. To cope with this problem, let's define the new state vector: $W^d=X^d-\Lambda_1U^d \Rightarrow zW^d=A^dX^d+\Lambda_0U^d$,

$$\Rightarrow\left\{\begin{array}{rcl} zW^d &=& A^dW^d+B^dU^d,\\ Y^d &=& C^dW^d+D^dU^d,\end{array}\right. \tag{23}$$

with $B^d=(A^d\Lambda_1+\Lambda_0)$, $C^d=C$ and $D^d=(C\Lambda_1+D)$.

To simplify notations, vectors and matrices of the discrete-time systems are renoted U, Y, X, A, B, C and D.

[1] For example, choosing the triangle approximation (modified first-order hold, cf. [18]), the coefficients of (20) are:
$\alpha_j=\mathrm{e}^{a_jT_s}$, $\lambda_{(j,0)}=-\frac{1-\alpha_j}{a_j^2T_s}-\frac{1}{a_j}$, and $\lambda_{(j,1)}=\frac{1-\alpha_j}{a_j^2T_s}+\frac{\alpha_j}{a_j}$.

4. REALIZABLE NETWORK

To build the network of a whole pipe, two-port systems of pieces of pipe (cf. Fig. 2) are connected together. This section is devoted to obtain a computationally realizable network of the whole system.

4.1. Concatenating systems

In Fig. 3 (top part), delay-free loops appear at interfaces of two systems which represent some cells of Fig. 2. These instantaneous loops cannot be simulated numerically as such, and it is necessary to remove them. To cope with this problem, it is possible to derive an equivalent two-port as the bottom of Fig. 3 shows.

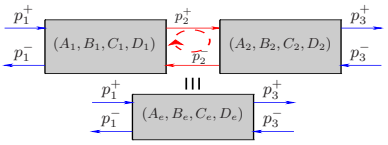

Figure 3: *Concatenating two two-ports*

In [11, p. 31-33], the interconnection laws are performed from state-space representations. This leads to the matrices A_e, B_e, C_e and D_e of the equivalent two-port. This operation is performed recursively to remove every instantaneous loop, until the network only contains intertwined two-port systems (without delay) and cells $\mathcal{Q}_P$ (with delay operators).

4.2. Minimal realization

At this stage of the building, a well-known result in automatic control allows to reduce the dimensions of the systems, in order to reduce the cost of numerical computation.

For an original state-space representation, the study of its observability allows to know if a change of state exists, which defines observable and *non-observable* sub-states. From an input/output point of view it is not necessary to simulate the last substates, because they have no influence on the output.

Similarly, the study of reachability allows to separate reachable and *unreachable* sub-states. With zero initial conditions, unreachable sub-states remain zero for bounded excitations U.

Using the canonical Kalman's form (cf. [19]), the *minimal realization* is derived by eliminating non-observable or unreachable sub-states. If they exist, the dimension of this minimal realization is lower than the original.

Remark: the minimal realization can be required for stability reasons in some particular cases (cf. eg. [20]).

4.3. Jordan decomposition

To reduce the calculation cost, it is useful to look for a new change of state which makes the matrix A sparse.

Considering the minimal realization of a system of the network, if its matrix A is diagonalizable over $\mathbb{C}^{J\times J}$, the modal form of the system is computed. If this matrix is not diagonalizable, it always admits a *Jordan* decomposition over $\mathbb{C}^{J\times J}$.

Then, the appropriate change of variable is done to lead to the new dynamics matrix A' with the diagonal form or the Jordan normal form. This matrix contains its complex eigenvalues on its diagonal, some 0 or 1 on its super-diagonal and 0 everywhere else.

4.4. Last reduction

Whereas all systems are real-valued (u_n and $y_n \in \mathbb{R}^N$), matrices of the state-space representation are complex-valued. From a numerical point of view, computation with complex numbers is more expensive than with real numbers. However using the hermitian symmetry of input/output transfer matrix ($\overline{H(s)} = H(\overline{s})$), it is possible to reduce the number of sub-states to calculate.

The matrix A is with the Jordan normal form, then its Jordan blocks are sorted with respect to their eigenvalues:

$$A' = \mathrm{diag}(A_{_R}, A_{_C}, A_{_{\overline{C}}}),$$

with $A_{_R}$ is a Jordan matrix composed with real eigenvalues, $A_{_C}$ is a Jordan matrix composed with complex eigenvalues with positive imaginary part, and $A_{_{\overline{C}}} = \overline{A_{_C}}$. Then $H(s)$ is decomposed:

$$H(s) = H_{_R}(s) + H_{_C}(s) + H_{_{\overline{C}}}(s) + D.$$

The hermitian symmetry of $H(s)$ and identifications prove that $\overline{H_{_R}(\overline{s})} = H_{_R}(s)$ and $\overline{H_{_C}(\overline{s})} = H_{_{\overline{C}}}(s)$. Thus, the contribution of $H_{_{\overline{C}}}(s)$ can be deduced from that of $H_{_C}(s)$.

Decomposing matrices with respect to eigenvalues of A', $B' = \left[B_{_R}, B_{_C}, B_{_{\overline{C}}}\right]^T$, $C' = \left[C_{_R}, C_{_C}, C_{_{\overline{C}}}\right]$ and $X' = \left[X_{_R}, X_{_C}, X_{_{\overline{C}}}\right]^T$, the equivalent scheme for simulation is, in time domain:

$$\begin{cases} \begin{bmatrix} x_{_R}(n+1) \\ x_{_C}(n+1) \end{bmatrix} = \begin{bmatrix} A_{_R} & \mathbf{0} \\ \mathbf{0} & A_{_C} \end{bmatrix} \begin{bmatrix} x_{_R}(n) \\ x_{_C}(n) \end{bmatrix} + \begin{bmatrix} B_{_R} \\ B_{_C} \end{bmatrix} u(n), \\ y(n) = C_{_R} x_{_R}(n) + 2\Re e\Big(C_{_C} x_{_C}(n)\Big) + Du(n). \end{cases}$$

5. RESULTS OF SIMULATIONS

From the geometry of a real trombone, two virtual trombones are built numerically. The varying cross-section pipe of the first virtual trombone, M_1, is built with 11 pieces of pipe, for a refined fit with the original shape of pipe. The second model, M_2, is a simplified version with 5 pieces of pipe. Additionally, the mouthpiece and the radiation impedance are modeled, but these models are not detailed here.

From the geometrical parameters of M_1 and M_2, the state-space representations of the networks of simulation are built with the procedures described in sections 3 and 4. These global systems which represent the resonator of a trombone, have one input and two outputs: the input is the incoming traveling wave p_e^+ at the entry of the mouth-piece, and their outputs are the traveling wave p_e^- outgoing from the mouth-piece and the radiated pressure p_s from the horn. Simulating the impulse response of the input reflexion of the resonator, p_e^-/p_e^+, in time domain, the computed input impedance, P/U, is deduced in frequency domain from (3).

Computed impedances are compared with the measured impedance of the real trombone[1] in Fig. 4. As we can see, the main improvement of the model M_1 (with 11 pieces of pipes) compared to that of M_2 (with 5 pieces) is about the spectral envelop. Whereas the envelop of maxima and minima of M_2 is smooth, that one of the measurements have some irregularities (see the fifth and the sixth maxima for example). With a best fit of the real shape of pipe, the envelop of M_1 has the same type of irregularities. However, because of the simplification of M_2, the complexity of the network of simulation is reduced.

[1] Measurements was done with the impedance sensor of the *Centre de Transfer de Technologie du Mans* (CTTM), Le Mans, France.

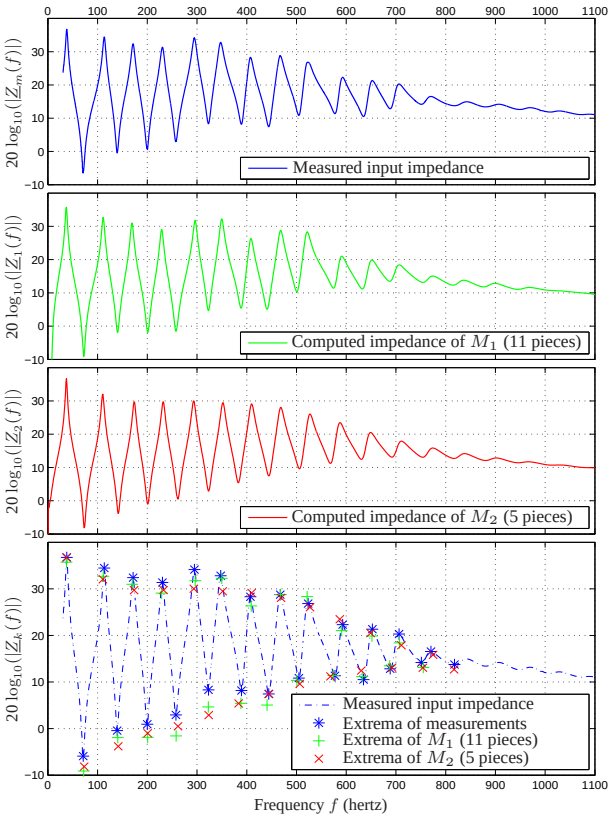

Figure 4: *Comparison between impedances.*

6. CONCLUSIONS AND PERSPECTIVES

Using the formalism of state-space representations for digital waveguide networks leads to a good modularity for the assembling of elements, and an automatic building of the network of simulation. Moreover, standard tools of automatic control are used to reduce the calculation cost.

Considering the refined model of *Webster-Lokshin* for lossy flared pipes, it has been shown that this formalism can be applied with approximations of the diffusive representations by finite-dimensional systems. Compared to models based on cylinders or cones, this model requires much fewer pieces of pipes to obtain good geometrical fits and realistic computed impedances.

At present, the global complexity of computation is equivalent to former models mentioned above. But the dimension of approximation (cf. sec. 3.1) can be reduced with a different method.

In this paper, only linear resonators with static parameters have been presented. In order to have a complete computer-aided maker of virtual wind instruments, nonlinear or time-varying system must be considered: trombone slide, valves, lips, reed, tone-holes. The modularity of the formalism should make an easy integration possible with only a few differences.

7. ACKNOWLEDGMENT

The authors thank René Caussé, Thomas Hézard and Pierre-Damien Dekoninck for their collaboration.

8. REFERENCES

[1] J. O. Smith, *Applications of Digital Signal Processing to Audio and Acoustics*, pp. 417–466, Kluwer Academic Publishers, February 1998.

[2] A. Webster, "Acoustic impedance and the theory of horns and of the phonograph," *Proc. Nat. Acad. Sci. U.S*, 1919.

[3] J. D. Markel and A. H. Gray, "On autocorrelation equations as applied to speech analysis," *IEEE Trans. Audio and Electroacoust.*, vol. AU-21, no. 2, pp. 69–79, April 1973.

[4] V. Välimäki, *Discrete-time modeling of acoustic tubes using fractional delay filters*, Ph.D. thesis, Helsinski University of Technology, 1995.

[5] D. Matignon, *Représentations en variables d'état de guides d'ondes avec dérivation fractionnaire*, Ph.D. thesis, Université Paris-Sud, 1994.

[6] E. Ducasse, "An alternative to the traveling-wave approach for use in two-port descriptions of acoustic bores," *J. Acoust. Soc. Am.*, vol. 112, pp. 3031–3041, 2002.

[7] J.-D. Polack, "Time domain solution of Kirchhoff's equation for sound propagation in viscothermal gases: a diffusion process," *J. Acoustique*, vol. 4, pp. 47–67, February 1991.

[8] T. Hélie, R. Mignot, and D. Matignon, "Waveguide modeling of lossy flared acoustic pipes: Derivation of a Kelly-Lochbaum structure for real-time simulations," in *IEEE WASPAA*, Mohonk, USA, 2007, pp. 267–270.

[9] T. Hélie, "Unidimensional models of acoustic propagation in axisymmetric waveguides," *J. Acoust. Soc. Am.*, 2003.

[10] D. Matignon, "Physical modelling of musical instruments: analysis/synthesis by means of state space representations," in *ISMA95*, pp. 496–502.

[11] S. Tassart, *Modélisation, simulation et analyse des instruments à vent avec retards fractionnaires*, Ph.D. thesis, Université Paris VI, Paris, 1999.

[12] R. Mignot, T. Hélie, and D. Matignon, "From the Webster-Lokshin equation to a general framework for simulation of digital waveguides," Submitted, 2009.

[13] T. Hélie, *Modélisation physique des instruments de musique en systêmes dynamiques et inversion*, Ph.D. thesis, Université Paris-Sud, Orsay, France, 2002.

[14] T. Hélie and D. Matignon, "Diffusive reprentations for the analysis and simulation of flared acoustic pipes with viscothermal losses," *Math. Models Meth. Appl. Sci.*, 2006.

[15] D. Matignon, "Stability properties for generalized fractional differential systems," *ESAIM: Proc*, vol. 5, 1998.

[16] O. J. Staffans, "Well-posedness and stabilizability of a viscoealistic in energy space," *Trans. Amer. Math. Soc.*, vol. 345, no. 2, pp. 527–575, 1994.

[17] G. Montseny, "Diffusive representation of pseudo-differential time-operators," *ESAIM: Proc*, vol. 5, 1998.

[18] G. F. Franklin, J. D. Powell, and M. L. Workman, *Digital Control of Dynamic Systems*, p.151, Addison-Wesley, 1990.

[19] R. Kalman, "Canonical structure of linear dynamical systems," in *Proc. of the Nat. Ac. of Sciences*.

[20] R. Mignot, T. Hélie, and D. Matignon, "Stable realization of a delay system modeling a convergent acoustic cone," in *MED08*.